Journal of Renewable Energies 24 (2021) 40 – 55 - **DOI:** https://doi.org/10.54966/jreen.v24i1.972

Journal of Renewable Energies
Revue des Energies Renouvelables
journal home page : https://revue.cder.dz/index.php/rer

Research Paper

Effect of cavity orientation on solidification/melting process of n-eicosane phase change material

Farida Iachachene [a,*]

[a] *Laboratoire Génie Physique des Hydrocarbures, Faculté des Hydrocarbures et de la Chimie, Université M'Hamed Bougara de Boumerdes, Avenue de l'Indépendance, 35000 Boumerdes, Algeria*

ARTICLE INFO

Article history:
Received 20 January 2021
Accepted 03 April 2021

Keywords:
CFD
Melting
Phase change material
Solidification
Orientation

ABSTRACT

In this paper, the melting and solidification of n-eicosane as a PCM inside two orientations of square containers is investigated numerically, using enthalpy–porosity method. The study reveals how the melting and solidification rate could be affected by changing the orientation of the phase change material container with a constant temperature boundary. It was found that the orientation of the square cavity has a significant effect on the melting and solidification rate of a PCM, the improvement is more than 40% for both cycles. Therefore the orientation of the heat exchange surface is a good control parameter for both the solidification and melting process

1. Introduction

Latent heat-based thermal energy storage is a favorable type of thermal energy storage system (TES) requiring smaller space, thanks to the large amount of energy needed to change the physical state of the material through a phase change. The phase change materials (PCM) should have high thermal conductivity for suitable charging and discharging rate [1].

---

* *Corresponding author, E-mail address: f.iachachene@univ-boumerdes.dz*

ISSN: 1112-2242 / EISSN: 2716-8247

One of the most commonly used PCMs in storing thermal energy is paraffin since it presents several advantages such as non-corrosiveness, low or no undercooling, possess chemical and thermal stability[2], the ability of congruent melting, self-nucleating properties, and compatibility with conventional materials of construction. However, low thermal conductivity, being around 0.2 W/m K, is the major drawback of latent thermal energy storage of paraffin, which decreases the melting/solidification rate and seriously limits their practical applications. Therefore, several techniques have been proposed to enhance heat transfer in PCMs such as using multiple PCMs [3], finned tubes [4], heat pipes [5], encapsulation parameters, namely, size (macro- to nano-encapsulation), shape, core-to-coating ratio, shell material and shell thickness [6], and dispersing highly conductive particles in PCM.

Considerable research work has been conducted on the performance of nanoparticle dispersed PCMs, known in the literature as nano-enhanced phase changed material (NEPCM) [7-12]. Almost all of these studies deduced that the NEPCM exhibits high heat transfer efficiency in comparison to the pure PCM, and consequently shortened the melting and solidification time.

Mother et al. [13] to examine detailed heat transfer characteristics of the melting process of n-Octadecane dispersed with TiO_2 nanoparticles in a rectangular enclosure performed an experimental investigation. They found that the incorporation of additives enhances the thermal conductivity but may suppress the natural convection mechanism. The natural convection suppression is attributed to the increase in the viscosity of the composite. This effect is dominant over the enhancement obtained in the thermal conductivity, with a resulting negative impact on the heat transfer rate.

There exist many experimental and numerical studies, which have revealed the significant role of buoyancy-driven convection heat transfer during the melting process of PCM in various configurations. The existence of natural convection during melting depends on the type of storage enclosure and its orientation.

Besides the NEPCM, the orientation of the PCM filled cavity can also have a substantial effect on the heat transfer characteristics of the PCMs. Kamkari et al. [14]studied a bottom-heated rectangular PCM container's melting behavior in three inclination angles. The melting time is found to be significantly shortened as the inclination angle increases from 0^o(vertical standing) to 90^o (horizontally placed), indicating strong heat transfer enhancement caused by natural convection. Arici et al. [15] undertook a numerical study on the melting of paraffin wax with Al_2O_3 nanoparticles in a partially heated and cooled square cavity. They illustrated that the heat energy stored by PCM can be enhanced by changing the orientation of thermally active walls of the enclosure, dispersing nanoparticles or applying both simultaneously. In the same context, Zeng et al. [16] investigated the PCM's melting process of lauric acid within a rectangular geometry at five different orientations. It was found that the melting time of PCM was significantly affected by changing the orientation of the heat exchange surface.

Dhaidan [17] also studied numerically the melting of n-eicosane as a PCM inside two orientations of triangular containers, where one storage cavity is a lower base container (LBC) and the other is the upper-base container (UBC). The results unfold that the melting rate is higher in the UBC than that in the LBC. In addition, it was found that the melting of the upper part of the container was higher than that recorded in the lower part for both orientations of the storage unit. Iachachene et al.[18] studied the orientation effect on the performance of the PCM embedded in a trapezoidal cavity. The effect of graphene nanoparticles was also examined. It was concluded that both effects are beneficial for heat transfer enhancements in PCMs. However, NEPCM leads to lower heat transfer performance when the nanofluid thermal conductivity enhancement was less than 80%. Recently, an experimental study was carried by Kalapala and Krishna [19] to analyze the effect of orientation of LHSU on the melting and solidification characteristics of PCM. They observed that the orientation has a major influence on the melting phenomenon and solidification is unaffected by the orientation of LHSU.

The objective of the present study is to examine the melting and solidification processes inside a square PCM at two orientations. The results are presented and discussed in terms of melting front, and melting rate.

2. Governing equations and physical Model

The dimensions and geometry of the computational model for the present study are shown in Fig. 1(a,b). The PCM is filled with a square cavity of size 1cm (a=1cm). The left wall is kept at a constant temperature. For the case of charge (melting), this temperature is higher than melting temperature (see fig 1(a)), and for the case of discharge (solidification), this temperature is lower than melting temperature (see fig 1(b)). The other sides are adiabatic.

The PCM considered for the present study is the paraffin n-eicosane The thermo-physical properties of PCM are represented in Table 1, inspired by Jones' work (Jones et al.[20]), assumed to be constant except for the density variation, which is approximated by the Boussinesq model.

The liquid PCM is assumed to be Newtonian and incompressible. The flow is laminar and the viscous dissipations, thermal radiation, and three-dimensional convection are negligible.

Considering the above mentioned assumptions, the governing equations for conservation of mass, momentum, and energy can be written as [21]:

$$\frac{\partial(\rho U)}{\partial t}+\frac{\partial(\rho V)}{\partial t}=0 \tag{1}$$

$$\frac{\partial(\rho U)}{\partial t}+\frac{\partial(\rho UU)}{\partial x}+\frac{\partial(\rho UV)}{\partial y}=-\frac{\partial P}{\partial x}+\frac{\partial}{\partial x}\left(\mu\frac{\partial U}{\partial x}\right)+\frac{\partial}{\partial y}\left(\mu\frac{\partial U}{\partial y}\right)+S_x \tag{2}$$

$$\begin{aligned}\frac{\partial(\rho V)}{\partial t}+\frac{\partial(\rho UV)}{\partial x}+\frac{\partial(\rho VV)}{\partial y}&=\frac{\partial P}{\partial y}+\frac{\partial}{\partial x}\left(\mu\ \frac{\partial V}{\partial x}\right)+\frac{\partial}{\partial y}\left(\mu\ \frac{\partial V}{\partial y}\right)\\&+(\rho\beta)g\left(T-T_m\right)+S_y\end{aligned} \tag{3}$$

$$\frac{\partial(\rho H)}{\partial t}+\frac{\partial(\rho UH)}{\partial x}+\frac{\partial(\rho UH)}{\partial y}=\frac{\partial}{\partial x}\left(k\frac{\partial T}{\partial x}\right)+\frac{\partial}{\partial y}\left(k\frac{\partial T}{\partial y}\right) \tag{4}$$

In the above equations, S represents the source term which is defined as [21]:

$$S_x=\frac{(1-f)^2}{f^3+\varepsilon}A_{mush}\,U\quad ,S_y=\frac{(1-f)^2}{f^3+\varepsilon}A_{mush}\,V \tag{5}$$

where ε=0.001 to prevent division by zero, A_{mush} is the mushy zone constant and *f* is the liquid volume fraction.

Table I. Thermophysical properties of n-eicosane Jones et al. [20]

Property	PCM solid	PCM liquid
Melting point T_f , C°	36.4	-
Density ρ, Kg/m^3	769	910
Specific heat C_p ,J/Kg k	1926	2400
Thermal conductivity *k* ,W/mK	0.423	0.146
Latent heat of fusion L_f ,J/kg	248000	-
Dynamic viscosity μ, Kg/ms	-	3,845 10-3
Thermal expansion coefficient β, K^{-1}	-	8,161 10-4

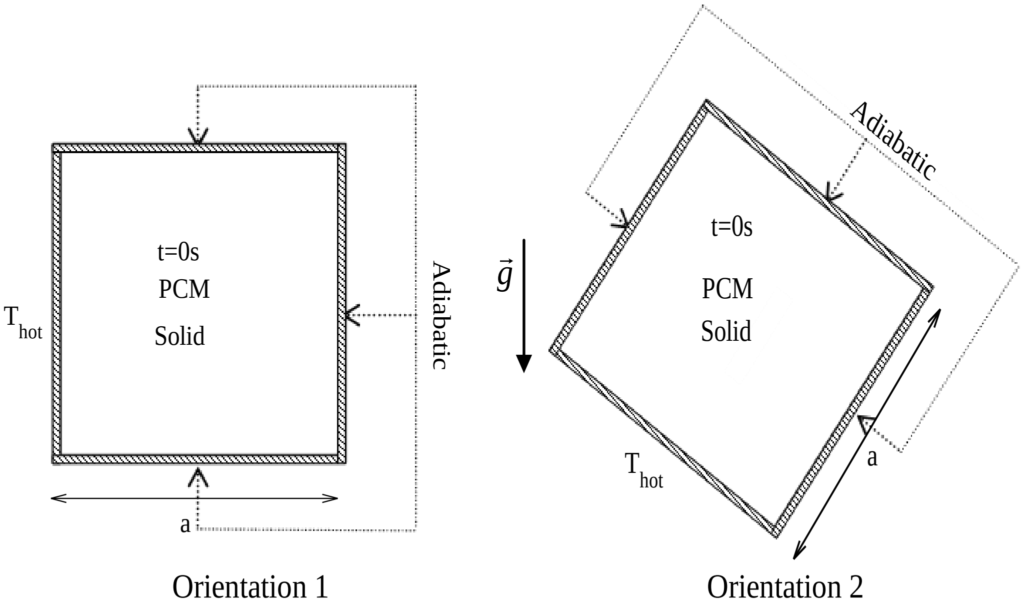

(a)- Melting

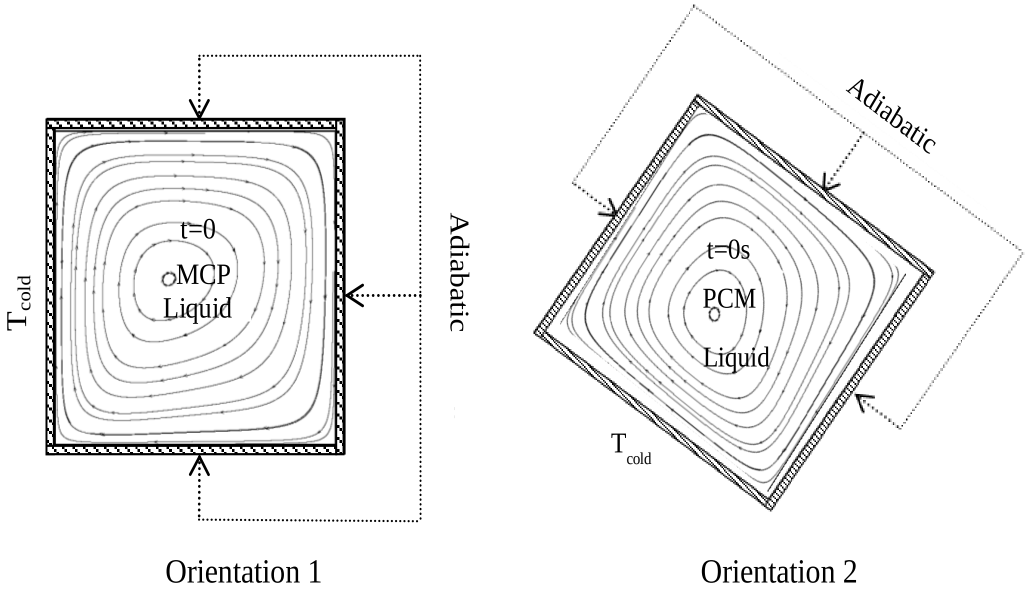

(b)- Solidification

Fig. 1. Physical model and boundary conditions

Enthalpy, H is the sum

$$H = h + \Delta H \tag{6}$$

$$h = h_{ref} + \int_{T_{ref}}^{T} c_p \, dT \tag{7}$$

$$\Delta H = f \, L_f \tag{8}$$

The enthalpy formulation requires a single domain in which the same set of governing equations are used to model both solid and liquid phases of a PCM. The transition from solid to liquid, and vice versa, occurs over a finite temperature range ($\Delta T_m = 0.5°C$) generating an artificial mushy region at the solid-liquid interface.

The fluid velocity within the mushy region varies from zero (at the solid boundary) to the natural convection velocity (at the liquid boundary) as the melt fraction varies from 0 to 1. In both cases, the phase change is quantified through the following equation for the melt fraction [21]:

$$f = \begin{cases} 0 & , T < T_{solidus} \\ \dfrac{T - T_{solidus}}{T_{liquidus} - T_s} & , T_{solidus} \leq T \leq T_{liquidus} \\ 1 & , T > T_{liquidus} \end{cases} \tag{9}$$

The thermophysical properties of PCMs are constants, but they differ for each phase as the temperature determines the PCM phases (solid, liquid, and mushy). Any general property G (maybe $\rho, k \, or \, c_p$) is defined according to the PCM phase as [17]:

$$G = \begin{cases} G_s & for\, solid\;\; PCM\;\; when\; , T < T_{solidus} \\ (1 - f)G_s + f\, G_l & for\, mushy\;\; zone\quad , T_{solidus} \leq T \leq T_{liquidus} \\ G_l & for\;\; fluid\;\; PCM\;\; when , T > T_{liquidus} \end{cases} \tag{10}$$

3. Numerical method and code validation

The solution of the Eqs. (1)–(4) has been done by the code software ANSYS -Fluent, which is based on the finite volume method. The thermophysical properties of phase change material are modeled using User Defined Function (UDF) according to the temperature, which determines the phase of PCMs.

Convective terms in momentum and energy equations are discretized using second order upwind interpolation scheme. The coupling between pressure and velocity is obtained by SIMPLE algorithm whereas PRESTO is adopted for pressure interpolation. The under-relaxation factors for the pressure correction, velocity components, thermal energy, and liquid fraction are 0.3, 0.7, 0.95, and 0.9, respectively. The convergence criteria are set at 10^{-6} for the continuity and momentum equations and at 10^{-10} for the energy equation. The time step is 0.1s, with a maximum of 500 iterations being performed along with the entire domain for each time step. The grid size and time step were chosen after careful examination of the independence of the results to these parameters. As shown in fig.2, the enclosure has meshed with a non-uniform rectangular grid with a very fine spacing near the walls.

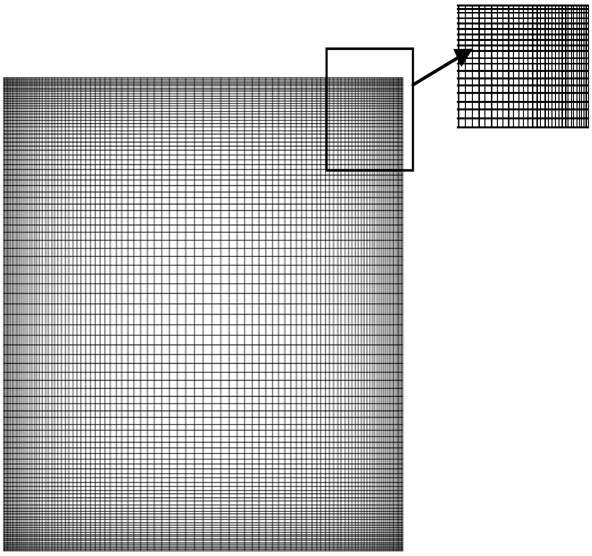

Fig. 2. Grid structure

An extensive mesh testing procedure was conducted to guarantee a grid-independent solution. Various mesh combinations of (80×80), (100×100), (120×120), and (200×200) cells were explored for the case $\Delta T = 20^{o}C$, it was found that no significant change in the results when using a finer mesh as shown in Fig. 3. In the present work, a grid size of (100×100) is employed.

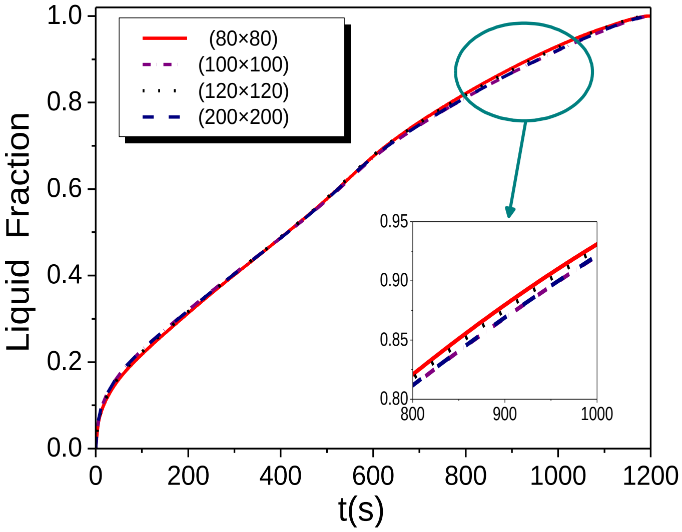

Fig. 3. Effects of grid size

The validation of the employed numerical approach can be confirmed by comparisons between the simulated results and the numerical/experimental data available in the literature. firstly, the computational model is validated against the experimental results of Gau and Viskanta [22] and the numerical predictions of Brent et al.[23] for a melting of Gallium in a rectangular enclosure at Pr = 0.0216, Ste = 0.039, and Ra = 6×10^5. Figure 4 shows the melt front of Gallium several times during the melting process. It can be seen that the present model predicts well the experimental data and is adequate for solid-liquid phase change problems with convection. The small discrepancy between the predicted melting interface of the present model and the experimental results may be explained by two possible reasons. First, it is difficult to ensure the heat and cold walls at a desired temperature in the experiment. Second, the three-dimensional effects are neglected. It was noticed that the difference between the variable and constant property results of Gallium were negligible.

In the second comparative analysis, the reliability of the current adopted model is tested through variations of liquid fraction from solidification of water in a square enclosure. As shown in Fig.5, It is clear that the present code is in good agreement with the reported numerical result of Sharma et al. [24].

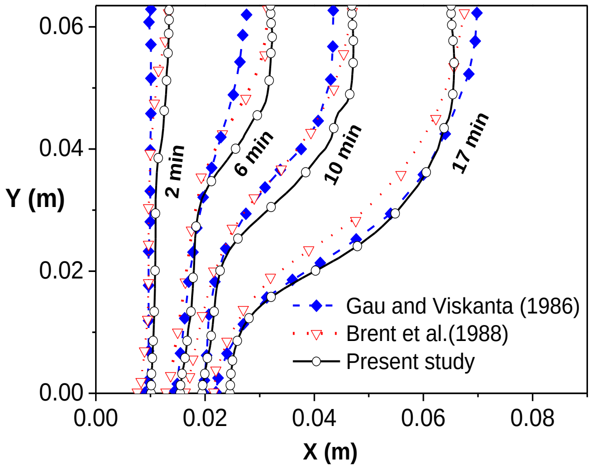

Fig. 4. Comparison of melting front at various times obtained by the present study and previously reported works.

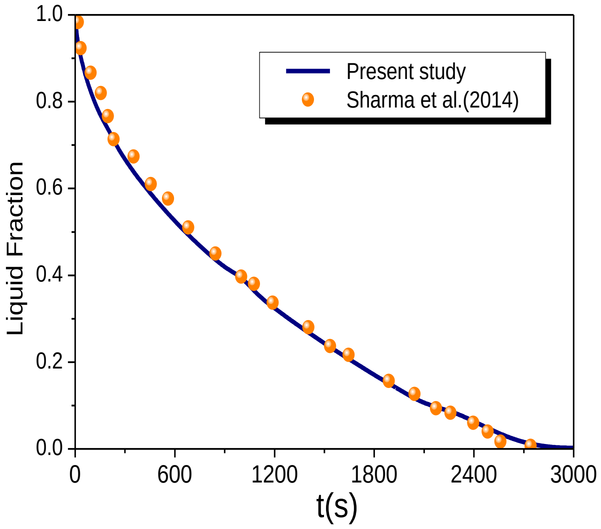

Fig. 5. Comparison of volume fraction profile from solidification between the present study and those of Sharma et al. [24].

4. Results and discussion

Detailed analysis on the development of the liquid-solid interface and liquid fraction of the PCM for the total melting and solidification processes will be presented in this section.

4.1 Progress of the solid-liquid interface

The progress of the position of the solid-liquid interface for$\Delta T = 20$ ° C was analyzed as time progresses. The contours of the liquid fraction at different melting and solidification stages for the two orientations are presented in fig 6 (a) and (b) respectively.

The comparison of the evolution of the solid-liquid interface, during the charge phase (melting) for the two considered orientations (fig 6(a)) leads to the following observations:

At the beginning ($t \leq$ 1mn) the molecular viscous force and conduction heat transfer are dominated as indicated by the melting interface being almost parallel to the hot wall both the two orientations.

Up to t = 3 min, the amount of melted paraffin is practically the same for both orientations. Natural convection begins to develop; the interface solid-liquid has a curvature in the upper part and remains vertical in the lower region.

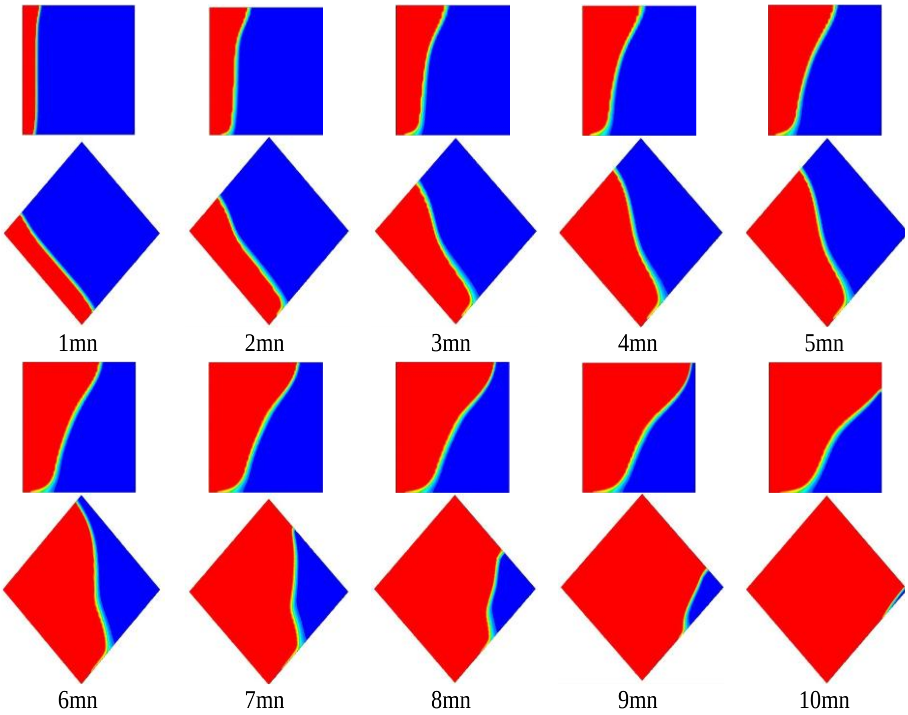

(a) Melting (charge) process

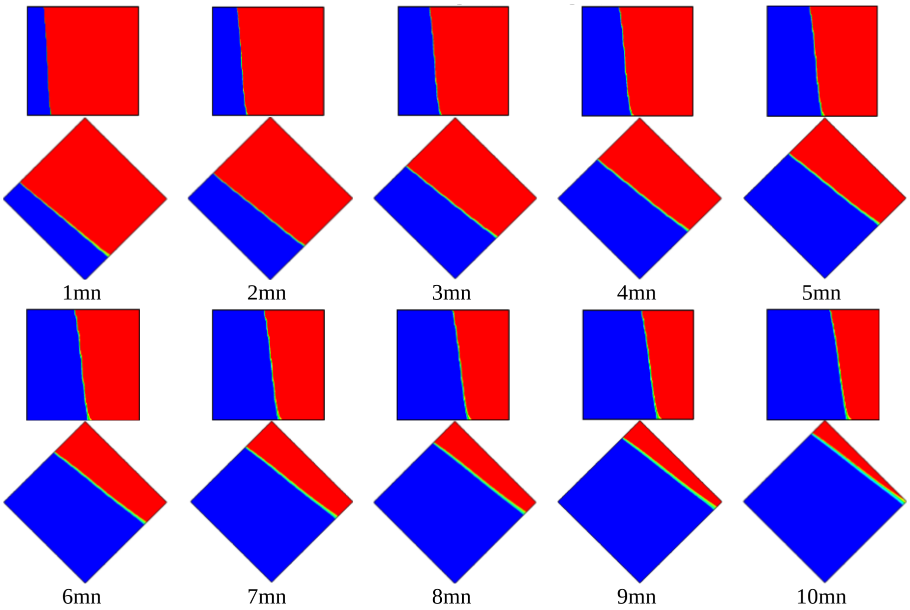

(b) Solidification (discharge) process,

Fig. 6. Motion of the solid-liquid interface:
(a) Melting (charge) process; (b) Solidification (discharge) process.

As the time elapses (t >3 mn), the entire interface is curved and moves faster in the upper than in the lower portion. This is due to the fact that the temperature of the PCM decreases as it flows down the solid-liquid interface, and the temperature gradients (and so the melting rates) are larger in the upper than in the lower portion of the enclosure. It is observed that the swiftness of fusion in orientation 2 is important than orientation 1.

This result indicates that the natural convection is more important in orientation 2, which leads to accelerating the heat transfer, why the melting occurs more quickly. Some authors have also reported the same results, where they found that the melting time of PCM could be significantly affected by simply changing the orientation of the cavity [9,17,18,19].

During a solidification process, see fig 6.b, the solid-liquid interface is almost parallel to the cold wall in both cases. At t = 1mn a layer of solidified PCM begins to form on the cold wall, this layer will isolate the liquid paraffin from the wall, so that the solidification continues slowly due to the poor thermal conductivity of the solid paraffin but also because of the small temperature difference between the interface solid and the liquid PCM. The shape of the phase front seems almost parallel to each other. This behavior is justified because convection does not have any role during the discharging process and conduction is solely responsible for the solidification of PCM. The comparison of the motion of solid-liquid interface both the two orientations indicates that the solidification is accelerated in orientation 2. however, Kalapala and Krishna [19] reported that the orientation had a minimal effect on the solidification process due to conduction dominated heat transfer.

From figures (6-a) and (6-b), we can deduce that the storage phase is faster than the destocking phase for both orientations. Because in the case of fusion natural convection promotes heat transfer. However, for the case of solidification, the heat transfer depends on the thermal conductivity of solid PCM which is relatively low.

4.2 Melt fraction

For a better insight into the melting process, the instantaneous liquid fraction of n-eicosane is shown in Fig. 7 for both orientations. Initially, the melting rate is high as the thermal energy is transferred by conduction through a thin thickness of liquid melt with lower thermal resistance and a high temperature gradient between the wall and a PCM. Also, it seems that the orientation of a cavity has no influence on the melt fraction at the initial periods of the melting process. Thereafter, the temperature gradient and associated heat transfer by conduction are reduced as the thickness of liquid melt increases which in turn causes growth in thermal resistance. But at the same time, natural convection will develop and compensates for degradation in conduction. Apparently, the temperature of the hot wall has a significant effect on the melting rate, and increasing it results in accelerating the melting process and shortening the melting time. For example, increasing ΔT from 20^0C to 30^0C will decrease the melting time by about 33% and 36% for orientations 1 and 2, respectively. Moreover, the melt fraction is higher for orientation 2 than that of orientation 1 for the same hot wall temperature. Utilizing orientation 2 instead of orientation 1 leads to savings in melting time by about 45,8%, 48.75%, and 41.66% for ΔT=20^0C, 30^0C, and 40^0C, respectively.

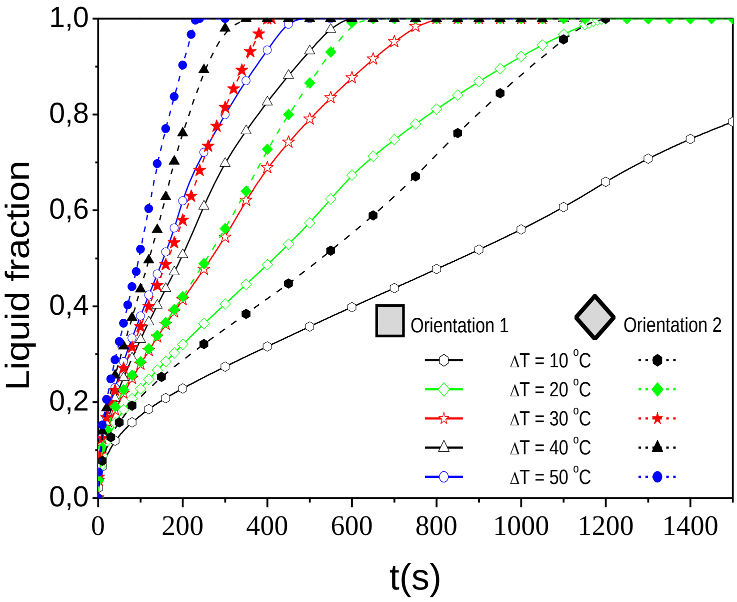

Fig. 7.Variations of liquid fraction with time at different temperature differences in melting case.

Figure 8 shows the liquid fraction versus time for different wall temperatures for both orientations and for the case of solidification. A lower wall temperature gives a larger solid fraction, which is obvious.

The solidification rate is large at the beginning of the solidification process. However, the solidification rate slows down as time increases. The thermal conductivity in the solid, and the temperature difference between the wall temperature and the melting temperature, are the main factors affecting the heat transfer process inside the enclosure.

We can observe that the solidification rate in orientation 2 is higher than in orientation 1 for the same cold wall temperature. Utilizing orientation 2 instead of orientation 1 leads to savings in solidification time by about 46.42%, 48.5%, and 40% for ΔT=20^0C, 30^0C, and 40^0C, respectively.

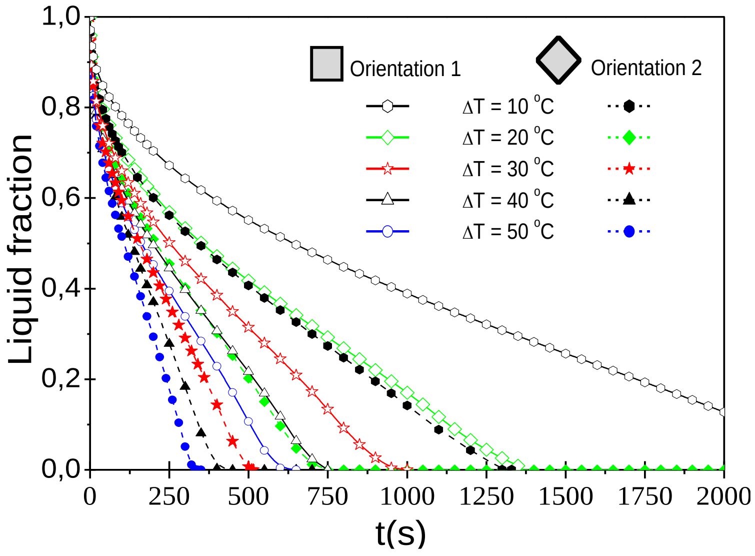

Fig. 8. Variations of liquid fraction with time at different temperature differences in solidification case.

5. Conclusion

The computational study of melting and solidification of n-eicosane PCM inside square heat storage units with two orientations is performed using the enthalpy-porosity method. The time-dependent variations of solid-liquid interface and melt fraction for both orientations of the cavity are investigated according to various temperatures of the hot wall. It was observed that the orientation of the square cavity has a significant effect on the melting and solidification rate of a PCM, the improvement is more than 40% for both cycles.

This result indicates that natural convection is more important in orientation 2 which leads to accelerating the heat transfer. Some authors have also reported the same results, where they found that the melting time of PCM could be significantly affected by simply changing the orientation of the cavity [14,19].

Then the orientation of the heat exchange surface (the storage unit) is a good control parameter for both solidification and melting process and it must be taken into account in practical engineering applications to reduce the time of charging and discharging in thermal storage devices.

Nomenclature:

a	Height of the cavity (m)	T	Temperature (K)
A_{mush}	Mushy zone constant (kg/m^3s)	T_f	Melting temperature (K)
C_p	Specific heat (J/kg·K)	x,y	Cartesian coordinates (m)
f	Liquid fraction	U,V	velocity components ($m \cdot s^{-1}$)
H	Sensible enthalpy (J/kg)		
h'	Latent heat ([J/kg)	**Greek symbols**	
k	Thermal conductivity (W/m·K)	μ	Dynamic viscosity (Ns/m^2)
L_f	Latent heat of fusion (J/kg)	ρ	Fluid density ($kg \cdot m^{-3}$)
P	Pressure (Pa)	**Subscript**	
Pr	Prandtl number	PCM	Phase change material
Q	Heat flux (W/m^2)	F	Fusion
t	Time (s)	S	Solid
S	Source term	L	Liquid

6. References

[1] Farid MM, Khudhair AM, Razack SAK, Al-Hallaj S. A review on phase change energy storage: materials and applications. Energ Covers Manage 2004; vol. 45, p. 1597–615.

[2] Gibbs BM, DSC Hasnain SM. Study of technical grade phase change heat storage materials for solar heating applications. Proceedings of the 1995; ASME/JSME/JSEJ international solar energy conference, Part 2.

[3] Fang M, Chen G. Effects of different multiple PCMs on the performance of a latent thermal energy storage system. Appl. Therm. Eng. 27, 2007; p. 994–1000.

[4] Al-Abidi AA, Mat S, Sopian K, Sulaiman MY, Mohammad ATh. Internal and external fin heat transfer enhancement technique for latent heat thermal energy storage in triplex tube heat exchangers. Appl. Therm. Eng. 53; 2013, p. 147–156.

[5] Sharifi N, Bergman TL, Allen MJ, Faghri A. Melting and solidification enhancement using a combined heat pipe. foil approach, Int. J. Heat Mass Transfer ,78 ;2014, p. 930–941.

[6] Salunkhe P, Shembekar PS. A review on effect of phase change material encapsulation on the thermal performance of a system. Renewable and Sustainable Energy Reviews 16; 2012, p. 5603–5616.

[7] Ranjbar AA, Kashani S, Hosseinizadeh SF, ghanbarpour M. Numerical heat transfer studies of a latent heat storage system containing nano-enhanced phase change material. Thermal science Vol. 15, No. 1; 2011, p. 169-181.

[8] Sebti SS, Mastiani M, Kashani S, Mirzaei H, Sohrabi A. Numerical study of melting an annular enclosure filled within nano-enhanced phase change material. Int. Therm. Sci. J.; 2013.

[9] Dhaidan NS, Khodadadi JM, Al-Hattab TA, Al-Mashat SM. Experimental and numerical investigation of melting of phase change material/nanoparticle suspensions in a square container subjected to a constant heat flux. International Journal of Heat and Mass Transfer 66; 2013, p. 672–683.

[10] Fan LW , Zhu ZQ , Zeng Y , Lu Q , Yu ZT. Heat transfer during melting of graphene-based composite phase change materials heated from below, “International Journal of Heat and Mass Transfer 79 ;2014, p. 94–104,

[11] Feng Y, Li H, Li L, Bu L, Wang T. Numerical investigation on the melting of nanoparticle-enhanced phase change materials (NEPCM) in a bottom-heated rectangular cavity using lattice Boltzmann method. Int. J. Heat Mass Transfer 81;2015,p. 415–425.

[12] Kant K, Shukla A, Sharma A, Biwole PH. Heat transfer study of phase change materials with graphene nanoparticle for thermal energy storage. Solar Energy 146; 2017, p. 453–463.

[13] Motahar S, Alemrajabi AA, Khodabandeh R. Experimental investigation on heat transfer characteristics during melting of a phase change material with dispersed TiO2 nanoparticles in a rectangular enclosure. Int J Heat Mass Transf, 2017; p.134–46.

[14] Kamkari B, Shokouhmand H, Bruno F. Experimental investigation of the effect of inclination angle on convection-driven melting of phase change material in a rectangular enclosure. Int J Heat Mass Transf; 2014, p.186–200.

[15] Arıcı M , Tütüncü M, Kan M, Karabay H. Melting of nanoparticle-enhanced paraffin wax in a rectangular enclosure with partially active walls. Int.J. Heat and Mass Transfer, 104;2017,p. 7–17.

[16] Zeng L, Lu J, Li1 Y, Li W, Liu S, Zhu J. Numerical study of the influences of geometry orientation on phase change material’s melting process. Advances in Mechanical Engineering;2017,Vol. 9(10), p. 1–11.

[17] Dhaidan NS. Melting phase change of n-eicosane inside triangular cavity of two orientations. Journal of renewable and substainable energy; 2017.

[18] Iachachene F, Haddad Z, Oztop HF, Abu-Nada E. Melting of phase change materials in a trapezoidal cavity: Orientation and nanoparticles effects. Journal of Molecular Liquids 2019; doi:10.1016/j.molliq.2019.03.051.

[19] Kalapala L and Devanuri J. K. Energy and exergy analyses of latent heat storage unit positioned at different orientations – An experimental study. Energy 2020; 116924. doi:10.1016/j.energy.2020.116924

[20] Jones B J, Sun D, Krishnan S, and Garimella S V.Experimental and numerical study of melting in a cylinder. Int. J.Heat Mass Transfer 49; 2006, p. 2724–2738.

[21] Haddad Z and Iachachene F. Melting characteristics of organic phase change material in a wavy trapezoidal cavity. Journal of Molecular Liquids 2019; https://doi.org/10.1016/j.molliq.2019.112132.

[22] Gau C, Viskanta R. Melting and Solidification of a Pure Metal on a Vertical Wall. J. Heat Transfer 108;1986, p. 174-181.

[23] Brent AD, Voller VR, Reid KJ. Enthalpy-porosity technique for modeling convection-diffusion phase change: application to the melting of a pure metal. Numer Heat Transfe13; 1988, p. 297–318.

[24] Sharma RK, Ganesan P, Sahu JN, Metselaar HSC, Mahlia TMI. Numerical study for enhancement of solidification of phase change materials using trapezoidal cavity.Powder Technol. 268;2014,p. 38–47.